Atlas-Based Recognition of Anatomical Structures and Landmarks to Support the Virtual Three-Dimensional Planning of Hip Operations

Jan Ehrhardt[1], Heinz Handels[1], Bernd Strathmann[2], Thomas Malina[1], Werner Plötz[2,3], and Siegfried J. Pöppl[1]

[1] Institute for Medical Informatics, University of Lübeck, 23538 Lübeck, Germany
[2] Department of Orthopedic Surgery, University of Lübeck, 23538 Lübeck, Germany
[3] Department of Orthopedic Surgery, Krankenhaus der Barmherzigen Brüder 80639 München, Germany

Abstract. This paper describes methods for the atlas-based segmentation of bone structures of the hip, the automatic detection of anatomical point landmarks and the computation of orthopedic parameters. An anatomical atlas was designed to replace interactive, time-consuming pre-processing steps needed for the virtual planning of hip operations. Furthermore, a non-linear gray value registration of CT data is used to recognize different bone structures of the hip. A surface based registration algorithm enables the robust and precise detection of anatomical point landmarks. Furthermore the determination of quantitative parameters, like angles, distances or sizes of contact areas, is important for the planning of hip operations. Based on segmented bone structures and detected landmarks algorithms for the automatic computation of orthopedic parameters were implemented. A first evaluation of the presented methods will be given at the end of the paper.

1 Introduction

During the computer supported 3D planning of hip operations anatomical structures like the head of the femur or the acetabulum have to be addressed in the virtual planning system. Furthermore, anatomical landmarks have to be determined to define a patient-related coordinate system and to compute orthopedic parameters, like angles or distances [1,2]. The interactive labeling of anatomical structures and landmarks is the most time-consuming pre-processing step and can take several hours. Hence, the automated recognition of anatomical structures and landmarks is a key problem for the virtual planning of operations and the construction of custom-made endoprostheses in practice. Three-dimensional digitized atlases of the pelvis are generated to support the virtual 3D-planning of hip operations. Starting point to built up the two atlases are the high resolution CT image sequences of the woman and the man of the Visible Human Data Set. Each atlas consists of labeled reference CT data sets, surface models of the

R.E. Ellis and T.M. Peters (Eds.): MICCAI 2003, LNCS 2878, pp. 17–24, 2003.

Fig. 1. Three-dimensional surface model of the female atlas data. The separated structures are visualized using different gray values. The landmarks are marked by points.

labeled anatomical structures and a set of anatomical landmarks. Figure 1 shows the surface models of the segmented bone structures and the associated landmarks. Non-linear, gray value-based and surface-based registration algorithms are presented, in order to make the automatic transfer of the atlas labels and landmarks to a patient data set possible. Beside the anatomical labeling of bone structures and landmarks the determination of orthopedic parameters, like angles, distances or sizes of contact areas, is important for the planning of hip operations. Thus, methods for the automatic computation of orthopedic measures were implemented.

2 Atlas-Based Segmentation of Bone Structures

A totally freeform registration process based on the "demons algorithm" [3] is used to transfer the atlas information to the patient's image data set. A multi-resolution strategy speeds up the computation and the convergence of the algorithm. But due to the strong anatomical variations in soft tissues a correct inter-patient matching of the whole pelvis region is nearly impossible. Therefore, in a first step a rough automatic segmentation of the patient's bones structures is applied using threshold based methods and morphological operators. For the coarse levels of the multi-resolution registration pre-segmented atlas and patient data sets are used. This leads to a fast and robust matching of the bone surfaces. In order to enable a good adjustment of internal bone structures and to be tolerant to errors of the threshold based segmentation, the original CT volumes are used at the finest resolution of the registration process. The results of the bone segmentation are used to restrict the demon positions to bone structures and surrounding voxels. By this technique the matching of non-corresponding soft tissue is avoided.

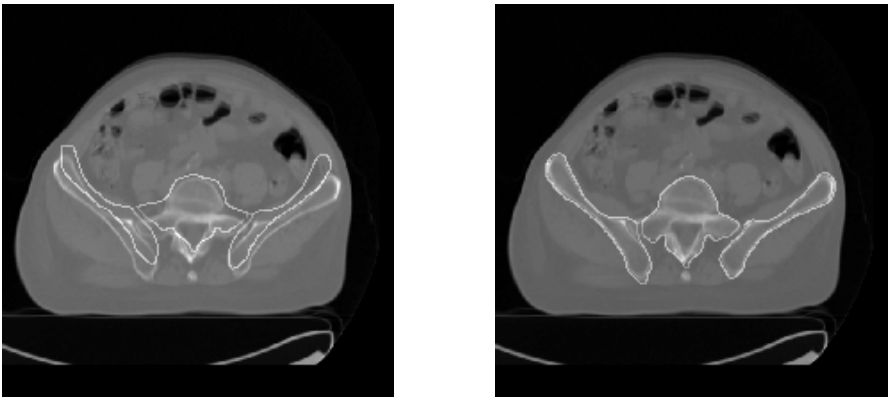

Fig. 2. CT slice of a patient's data set superimposed with the edges of the atlas bone structures (white) before (left) and after the non-rigid registration (right).

In figure 2 the 3D registration is illustrated by a CT slice of a patient's data set superimposed with the contours of the atlas bone structures before and after the freeform registration. A good fit of atlas and patient data is obtained finally, but nevertheless small deviations can occur.

The atlas information is transferred by means of a nearest-neighbor approach to the patient data. Based on the threshold segmentation of the patient's bone structures the label of the nearest structure in the transformed atlas data set is assigned to each segmented voxel. Thus, bony patient voxels, which are not covered by an atlas label, are added to the nearest bone structure.

3 Atlas-Based Determination of Anatomical Landmarks

By the presented gray value registration process the anatomical landmarks can be transferred from the atlas to the patient data. But inaccuracies of the atlas-patient registration are introduced by varying anatomical details and gray values (e.g. due to different calcification of bones) and by smoothness constraints of the deformation field. Hence the automatic determined landmarks can differ strongly from the correct positions.

Therefore a new surface-based registration method has been developed to allow the robust and precise transfer of anatomical landmark positions from the atlas to the patient data. In a first step, surface models of the bone structures of the patient are generated using the *Marching-Cubes* algorithm. In order to compute an improved position of the patient's landmark, a non-linear matching of the atlas surface model and the patient's surface model in a local environment of the landmark is performed (see Fig. 3). Denotes $\mathcal{A}$ the triangulated surface of the atlas structure, $\boldsymbol{l}_{\mathcal{A}}$ the position of an atlas landmark, $\mathcal{P}$ the patient's

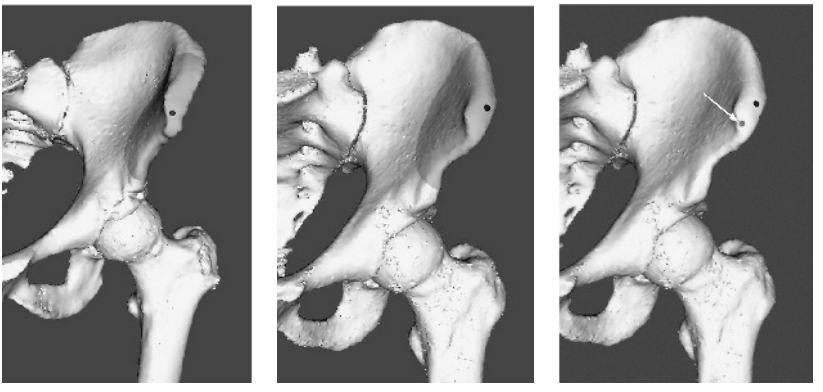

Fig. 3. The surface model of the anatomical atlas with one anatomical landmark (left) and the surface model of a patient with the initial landmark position (middle). The locale surface cut-outs are displayed as colored areas. Right the automatically corrected position of the patient's landmark is marked with an arrow.

bone surface and $\hat{\boldsymbol{l}}_{\mathcal{P}}$ the initial landmark position determined by the gray value registration. The applied procedure can be described as follows:

1. Let $\boldsymbol{l}_{\mathcal{P}}^0 = \hat{\boldsymbol{l}}_{\mathcal{P}}$ and $k = 0$.
2. Generate a local cut-out $\tilde{\mathcal{A}}$ with center $\boldsymbol{l}_{\mathcal{A}}$ and a local cut-out $\tilde{\mathcal{P}}^k$ with center $\boldsymbol{l}_{\mathcal{P}}^k$ of the surface models:

$$\tilde{\mathcal{P}}^k = \left\{ \boldsymbol{T}_j \in \mathcal{P} \,|\, \|\boldsymbol{c}(\boldsymbol{T}_j) - \boldsymbol{l}_{\mathcal{P}}^k\| < r \right\} \text{ and}$$
$$\tilde{\mathcal{A}} = \left\{ \boldsymbol{T}_j \in \mathcal{A} \,|\, \|\boldsymbol{c}(\boldsymbol{T}_j) - \boldsymbol{l}_{\mathcal{A}}\| < r \right\}.$$

   $\boldsymbol{T} \in \mathcal{A}$ (resp. $\boldsymbol{T} \in \mathcal{P}$) denotes a triangle of the surface $\mathcal{A}$ (resp. $\mathcal{P}$) and $\boldsymbol{c}(\boldsymbol{T})$ is the center of the triangle $\boldsymbol{T}$. The size of the cut-out is given by a radius r.
3. An affine transformation $\boldsymbol{\phi}_1^k$, which matches $\tilde{\mathcal{A}}$ and $\tilde{\mathcal{P}}^k$ as well as possible is determined using the *Iterative-Closest-Point* algorithm (ICP).
4. A nonlinear transformation $\boldsymbol{\phi}_2^k$ is determined by means of the so-called *Geometry-Constrained-Diffusion* (GCD) [4] in order to adapt the pre-registered surfaces.
5. Compute the new position of the patient's landmark

$$\boldsymbol{l}_{\mathcal{P}}^{k+1} = (\boldsymbol{\phi}_2^k \circ \boldsymbol{\phi}_1^k)(\boldsymbol{l}_{\mathcal{A}}).$$

6. If the stop criterion is not fulfilled, set $k = k + 1$ and go to 2.

The most important parameter of the procedure is the radius r, which specifies the size of the regarded local surface area. If the radius is chosen too small, the surface characteristics in the environment of a landmark cannot be captured. If the radius is chosen too large, only an insufficient registration result can be

achieved due to the patient-specific variations. In our application the parameter r decreases during the registration process. The initial size of the radius is determined empirically for each landmark.

The differential characteristics of the surfaces contain important information about the correspondence of surface points. Therefore the surface normals and local curvature characteristics are considered in the context of the linear and non-linear registration processes. Central task of the ICP and GCD algorithm is the iterative determination of corresponding points between the source surface $\tilde{\mathcal{A}}$ and the target surface $\tilde{\mathcal{P}}^k$. Normally, only a nearest neighbor approach based on the Euclidean distance of the points is used. In our application the computed normal vectors and curvature characteristics are used in the registration algorithms too: For every point $\boldsymbol{p}$ on the deformed surface $\tilde{\mathcal{A}}$ find the corresponding point $\boldsymbol{q}$ on the target surface $\tilde{\mathcal{P}}^k$, which minimizes:

$$D(\boldsymbol{p},\boldsymbol{q}) = \alpha\|\boldsymbol{p}-\boldsymbol{q}\|^2 + \beta\|\boldsymbol{n}(\boldsymbol{p})-\boldsymbol{n}(\boldsymbol{q})\|^2 + \gamma(\kappa_\epsilon(\boldsymbol{p})-\kappa_\epsilon(\boldsymbol{q}))^2. \tag{1}$$

$\boldsymbol{n}(\boldsymbol{p})$ denotes the surface normal and $\kappa_\epsilon(\boldsymbol{p})$ denotes a curvature value of point $\boldsymbol{p}$. *Kd-trees* are used to perform an efficient search. The normal vectors $\boldsymbol{n}$ of the triangulated surface models are calculated as proposed in [5]. Due to the faceted nature of triangulated surface models, the curvature computation has to deal with discontinuities at edges and vertices. Classical algorithms for the determination of surface curvature calculate the curvature between neighboring triangles [6,7]. These algorithms are not independent of the size of the triangles. If the underlying CT data of atlas and patient have different resolutions, the application of these algorithms leads to unsatisfactory results. To avoid these problems, a new curvature measure of discrete surfaces κ_ϵ is used (see [8] for details). First, the barycentre $\boldsymbol{S}_\epsilon(\boldsymbol{x})$ of a small neighborhood of the surface point $\boldsymbol{x}$ is determined. Then the distance

$$\kappa_\epsilon(\boldsymbol{x}) = \frac{1}{\epsilon}\left(\boldsymbol{n}(\boldsymbol{x})\cdot(\boldsymbol{S}_\epsilon(\boldsymbol{x})-\boldsymbol{x})\right) \tag{2}$$

between $\boldsymbol{S}_\epsilon(\boldsymbol{x})$ and the tangential plane through the point $\boldsymbol{x}$ with surface normal $\boldsymbol{n}(\boldsymbol{x})$ is computed. The size of the regarded neighborhood is given by the built-in scale parameter ϵ. In our application we chose $\epsilon = 5mm$ for all surfaces. The curvature measure κ_ϵ allows to distinguish smooth regions ($\kappa_\epsilon \approx 0$) from convex surface regions ($\kappa_\epsilon < 0$) and from concave surface regions ($\kappa_\epsilon > 0$). The presented method is an extension of the curvature classification via local zero order moments as suggested in [9].

4 Automatic Computation of Orthopedic Parameters

The determination of orthopedic parameters, e.g. distances or angles, is very important for the diagnosis and treatment as well as for the long-term operation result in orthopedic surgery. A list of orthopedic parameters needed for the planning of hip operations was provided by the involved surgeons, and a software tool for the automatic computation of these parameters was developed. Most of

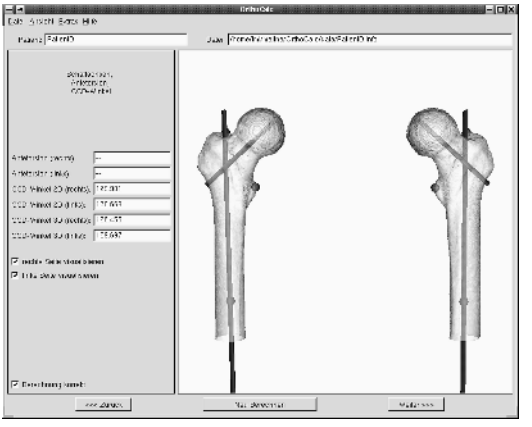

Fig. 4. Visualization of the axis of the femoral leg and the femoral neck of a patient's data set with the program `OrthoCalc`.

these orthopedic parameters were defined based on 2D x-ray projections. Thus, new 3D computation methods for orthopedic parameters were needed.

The program `OrthoCalc` calculates the desired parameters automatically based on the segmented patient data set, the 3D models of the different bone structures and the associated anatomical landmarks. First, a patient-related coordinate system is determined by symmetrical point landmarks. Afterwards numerous orthopedic parameters are calculated, e. g. the anteversion and inclination of the hip joint, the CE-angle, the CCD-angle and the antetorsion of the femur. For example, the computation of the CE-angle requires the determination of the center of the femoral head and of the edge of the acetabulum. The center is determined using a sphere approximation of the femoral head. Starting from the computed center a ray-tracing algorithm is used to find the edge of the acetabulum. This edge can also be used to calculate the anteversion and inclination of the hip joint.

Furthermore, new three-dimensional orthopedic parameters can be calculated. For example the color-coded visualization of the distance between the femoral head and the acetabulum enables the surgeon to evaluate the contact area of the hip joint. Figure 4 shows the user interface of the implemented program. The automatically determined axis of the femoral neck and of the femoral shank are displayed, on which the calculation of the CCD-angle and the antetorsion is based.

5 Results

The atlas based recognition of bone structures was evaluated by matching the atlas data sets and the CT data of seven patients with a resolution of about

$0.7 \times 0.7 \times 4mm^3$. In a first step, the image volumes of atlas and patient were resliced to an iso-voxel resolution of $2 \times 2 \times 2mm^3$ due to memory and runtime issues. To obtain a good starting position an affine pre-registration was performed. The gray value based freeform registration described in section 2 was used to match the atlas and patient's CT volumes. Following the atlas labels were transferred to the patient data sets. The results of the atlas-based recognition method were compared with manual segmentation results. 98.5% of the bony voxels were labeled correctly on average. The high recognition rate indicates that several bone structures can be segmented with sufficient accuracy. But, post-processing algorithms are needed to guarantee and to improve the recognition quality in the area of the acetabulum, which is of high importance for the construction of individually adapted endoprostheses [2]. For two patient data sets an interactive correction of the segmentation of the femoral head was necessary due to pathological deformations of the hip joint. Furthermore, partial volume effects, which are caused by the low z-resolution of the patient data sets, prevent the correct recognition of the upper part of the hip joint. Therefore, for all patient data sets an interactive correction of 2-4 slices was necessary to obtain a good segmentation of the hip joint. However, preliminary tests indicate better results for CT data with a higher spatial resolution.

Furthermore, initial landmark positions of the patient data sets were determined by the gray value based registration. These positions can deviate significantly (up to $10mm$) from the correct landmark localizations due to the inaccuracies of the gray value registration. In order to enable a precise computation of orthopedic measures the correction of these landmark positions is necessary. For this purpose the surface based registration method described in section 3 was used to correct the position of 20 anatomical landmarks of the hip for the seven patient data sets. A visual control of the detected landmarks results in that all patient landmarks were correctly positioned. In a second step the independence of the presented landmark correction method of the initial landmark positions was tested. Therefore, a set of 25 randomly chosen initial landmark positions was generated with a maximum distance of $10mm$ to the correct landmark position. Afterwards for everyone of these starting positions the surface registration was executed. The mean distance of the automatically corrected landmark positions to their average value was below $1mm$ and the maximum distance was below $3mm$. The small deviations indicate that for all initial positions approximately the same final landmark position was obtained, but due to a suboptimal choice of the radius r distances of up to $3mm$ can occur for single data sets.

The automatic determination of orthopedic parameters has been applied to the two atlas data sets and five manually segmented patient data sets. All orthopedic parameters could be computed in the two atlas data sets but only in three patient data sets. In one case the edge of the acetabulum was not identified, due to a bone tumor and in the other case the center of the femoral head could not be computed due to a strong pathological deformation of the hip joint. A qualitative and quantitative evaluation of the system takes place at present in a clinical study.

6 Conclusion

We have presented an anatomical atlas to support the virtual three-dimensional planning of hip operations, consisting of segmented bone structures and a set of anatomical point landmarks. A gray value registration algorithm for the automatic transfer of the atlas information to patient data was implemented. A surface based registration method enables reliable and precise detection of anatomical landmarks. In comparison to other methods (see e.g. [10]) the anatomical landmarks are not limited to positions with extreme differential characteristics and no user interactions are necessary. The software tool `OrthoCalc` was developed to enable the automatic calculation of orthopedic parameters. A first evaluation of the presented methods shows promising results.

The atlas-based segmentation of bone structures, the atlas-based landmark detection and the automatic computation of orthopedic measures are suitable to reduce the time-consuming user interaction during the preprocessing of the CT data for the virtual 3D planning of hip operations, significantly.

Currently, we develop post-processing algorithm using active contour models [11] to segment the acetabulum and the femoral head with improved accuracy.

References

1. DiGioia, A.M., et al.: Hipnav: pre-operative planning and intra-operative navigational guidance for acetabular implant placement in total hip replacement surgery. In: Proc. of Computer Assisted Orthopedic Surgery, Bern (1995)
2. Handels, H., Ehrhardt, J., Strathmann, B., Pl tz, W., P ppl, S.: Three-dimensional planning and simulation of hip operations and computer-assisted design of endoprostheses in bone tumor surgery. J. of Comp. Aided Surg. **6** (2001) 65–76
3. Thirion, J.P.: Image matching as a diffusion process: an analogy with maxwell's demons. Medical Image Analysis **2** (1998) 243–260
4. Andresen, P.R., Nielsen, M.: Non-rigid registration by geometry–constrained diffusion. Medical Image Analysis **5** (2001) 81–88
5. Schroeder, W.J., Martin, K., Lorensen, W.E.: The Visualization Toolkit. 2nd edn. Prentice Hall (1998)
6. Smith, A.D.C.: The folding of the human brain: from shape to function. PhD thesis, University of London (1999)
7. Desbrun, M., Meyer, M., Schr der, P., Barr, A.: Implicit fairing of irregular meshes using diffusion curvature flow. In: SIGGRAPH 99. (1999) 317–324
8. Ehrhardt, J., Handels, H., P ppl, S.J.: Atlas-based determination of anatomical landmarks to support the virtual planning of hip operations. In: CARS 2003, Elseviewer (2003)
9. Clarenz, U., Dziuk, G., Rumpf, M.: On generalized mean curvature flow. In Hildebrandt, S., Karcher, H., eds.: Geometric Analysis and Nonlinear Partial Differential Equations, Springer (2003)
10. Frantz, S., Rohr, K., Stiehl, H.S.: Improving the detection performance in semiautomatic landmark extraction. In: Proc. MICCAI'99. LNCS 1679, Springer (1999)
11. M. Kass, A.W., Terzopoulos, D.: Active contour models. In: IEEE Proc. of First Int. Conf. on Comp. Vision, London (1987) 259–269